Computational Study of the Release of H2 from Ammonia Borane Dimer (BH3NH3)2 and Its Ion Pair Isomers

5 AUTHORS, INCLUDING:

Nguyen Vinh Son
University of Leuven
35 PUBLICATIONS   490 CITATIONS

Minh Tho Nguyen
University of Leuven
748 PUBLICATIONS   10,861 CITATIONS

David A Dixon
University of Alabama
767 PUBLICATIONS   22,217 CITATIONS

Computational Study of the Release of H$_2$ from Ammonia Borane Dimer (BH$_3$NH$_3$)$_2$ and Its Ion Pair Isomers

Vinh Son Nguyen,[†] Myrna H. Matus,[‡] Daniel J. Grant,[‡] Minh Tho Nguyen,*,[‡,†] and David A. Dixon*,[‡]

Department of Chemistry, University of Leuven, B-3001 Leuven, Belgium, and Department of Chemistry, The University of Alabama, Shelby Hall, Tuscaloosa, Alabama 35487-0336

High-level electronic structure calculations have been used to map out the relevant portions of the potential energy surfaces for the release of H$_2$ from dimers of ammonia borane, BH$_3$NH$_3$ (**AB**). Using the correlation-consistent aug-cc-pVTZ basis set at the second-order perturbation MP2 level, geometries of stationary points were optimized. Relative energies were computed at these points using coupled-cluster CCSD(T) theory with the correlation-consistent basis sets at least up to the aug-cc-pVTZ level and in some cases extrapolated to the complete basis set limit. The results show that there are a number of possible dimers involving different types of hydrogen-bonded interactions. The most stable gaseous phase (**AB**)$_2$ dimer results from a head-to-tail cyclic conformation and is stabilized by 14.0 kcal/mol with respect to two **AB** monomers. (**AB**)$_2$ can generate one or two H$_2$ molecules via several direct pathways with energy barriers ranging from 44 to 50 kcal/mol. The diammoniate of diborane ion pair isomer, [BH$_4$$^-$][NH$_3BH_2NH_3$$^+$] (**DADB**), is 10.6 kcal/mol less stable than (**AB**)$_2$ and can be formed from two **AB** monomers by overcoming an energy barrier of ~26 kcal/mol. **DADB** can also be generated from successive additions of two NH$_3$ molecules to B$_2$H$_6$ and from condensation of **AB** with separated BH$_3$ and NH$_3$ molecules. The pathway for H$_2$ elimination from DADB is characterized by a smaller energy barrier of 20.1 kcal/mol. The alternative ion pair [NH$_4$$^+$][BH$_3NH_2BH_3$$^-$] is calculated to be 16.4 kcal/mol above (**AB**)$_2$ and undergoes H$_2$ release with an energy barrier of 17.7 kcal/mol. H$_2$ elimination from both ion pair isomers yields the chain BH$_3$NH$_2$BH$_2$NH$_3$ as product. Our results suggest that the neutral dimer will play a minor role in the release of H$_2$ from ammonia borane, with a dominant role from the ion pairs as observed experimentally in ionic liquids and the solid state.

Introduction

There is considerable interest in the development and application of hydrogen-based fuel cells as a viable alternative energy source based on renewable fuels. A critical issue with hydrogen as a fuel for use in on-board transportation systems is the need to find efficient chemical H$_2$ storage materials that enable the safe and efficient release/uptake of H$_2$.[1] Ammonia borane (BH$_3$NH$_3$, **AB**)[2−4] and its derivatives have recently emerged as promising hydrogen sources.[5−11] Using high accuracy ab initio electronic structure theory calculations of reaction thermodynamic parameters, in both the gas phase and the solid state, we have shown that molecular **AB** and the corresponding salt [BH$_4$$^-$][NH$_4$$^+$] can serve as good hydrogen storage systems that release H$_2$ in slightly exothermic processes.[6] The isovalent systems including alane amine (AlH$_3$NH$_3$), borane phosphine (BH$_3$PH$_3$), and phosphine alane (AlH$_3$PH$_3$) and their corresponding salts [XH$_4$$^-$][YH$_4$$^+$], with X = B or Al and Y = N or P, have also been shown to possess appropriate thermodynamic properties to serve as H$_2$ storage systems.[7]

The potential of a compound for chemical hydrogen storage is dependent on the inherent kinetics and mechanism of the processes releasing H$_2$ and regenerating the compound that stores H$_2$. Using thermo-analytical techniques, Wolf and co-workers[5] found that **AB** begins to undergo stepwise thermal decompositions at temperatures as low as 410 K. During the first decomposition step, approximately 1 mol of H$_2$ per mole of **AB** is released, together with aminoborane (BH$_2$NH$_2$), and other polymeric derivatives. Subsequent quantum chemical calculations[12] using various composite methods suggested that formation of the first H$_2$ from an **AB** molecule occurs through a concerted mechanism characterized by a planar four-membered transition structure with an energy barrier of around 32−33 kcal/mol. In a recent much higher-level computational study,[13] we showed that, in its monomeric form, **AB** undergoes preferentially B−N bond cleavage giving BH$_3$ and NH$_3$. In fact, at the CCSD-(T)/complete basis set (CBS) level of theory, the B−N bond dissociation energy of 26 kcal/mol is smaller than the energy barrier of 37 kcal/mol for the concerted H$_2$ elimination. With a difference of 11 kcal/mol in barrier heights, the thermal decomposition of **AB** is dominated by the bond cleavage channel. Under these conditions, H$_2$ formation is not competitive, inconsistent with the experimental results mentioned above. We showed that a borane molecule could effectively act as a bifunctional Lewis acid catalyst favoring H$_2$ formation from **AB**. With BH$_3$ formed by breaking the B−N bond in **AB**, the corresponding energy barrier is thus reduced to about 6 kcal/mol with respect to the BH$_3$NH$_3$ + BH$_3$ separated reactants.[13] These results show that without a catalyst the rate of H$_2$ release from the **AB** monomer is very low at low temperatures. We note that the starting **AB** materials exist as a solid.

* Author to whom correspondence should be addressed. E-mail: dadixon@bama.ua.edu.
  † University of Leuven.
  ‡ The University of Alabama.

Release of H$_2$ from (BH$_3$NH$_3$)$_2$

J. Phys. Chem. A, Vol. 111, No. 36, 2007 **8845**

TABLE 1: Relative Energies (kcal/mol) of Ammonia Borane Dimer and Its Ion Pair Isomers Calculated at the CCSD(T) Level with Different Basis Sets[a]

structure	aVDZ	aVTZ	aVQZ	CBS
dim	0.0	0.0	0.0	0.0
DADB	10.6	10.7	10.6	10.6
IonP-N	16.5	16.6	16.5	16.4

[a] Using the aug-cc-pVnZ basis sets, with n = D, T, and Q, and extrapolated CBS energies. Relative energies include zero-point corrections obtained from MP2/aVDZ harmonic vibrational frequencies scaled by a factor of 0.9751.

TABLE 2: Relative Energies (kcal/mol) of Stationary Points Related to H$_2$ Release from Ammonia Borane Dimers dim and DADB Calculated at the CCSD(T) Level with Different Basis Sets[a]

structure	aVDZ	aVTZ	aVQZ	CBS
2**AB**	0.0	0.0	0.0	0.0
dim	−14.2	−14.0	−13.7	−13.5
dim-ts1	36.3	36.0	35.9	35.9
dim-p1 + 2H$_2$	−13.8	−15.4	−16.0	−16.4
2(BH$_2$NH$_2$) + 2H$_2$	−10.7	−12.6	−13.5	−14.0
DADB	−3.5	−3.3	−3.0	−2.8
DADB-ts1	17.2	17.2	17.2	17.3
DADB-p1 + H$_2$	−7.8	−9.3	−9.4	−9.3

[a] On the basis of CCSD(T) energies using MP2/aVTZ-optimized geometries and ZPE corrections from scaled MP2/aVDZ harmonic vibrational frequencies.

It has experimentally been found that "seeding" of **AB** results in significantly faster H$_2$ production. The seed compound has been proposed to be the diammoniate of diborane [BH$_4^-$] [NH$_3$BH$_2$NH$_3^+$] (**DADB**), an ion pair isomer of the (**AB**)$_2$ dimer.[14] Recent in situ solid-state ^{11}B magic-angle spinning NMR studies[15] at 88 °C demonstrated that during the thermal decomposition of **AB** to produce H$_2$ **DADB** is present. These authors suggested that the formation of **DADB** is the prerequisite for H$_2$ release. In ionic liquids containing **AB**, the formation of **DADB** was also observed.[8b] These authors also suggested an important role for **DADB** in H$_2$ release noting that there was no induction period for H$_2$ release in the ionic liquid whereas there was an induction period in the pure solid. The ionic liquid would favor the formation of ionic intermediates such as **DADB**. It has been reported that **DADB** produces polyaminoborane upon heating[16] and that polyaminoboranes were observed in the ionic liquid as H$_2$ was released. Another starting point connecting to the ion pair is that of diborane and two ammonia molecules (B$_2$H$_6$ + 2NH$_3$).[17] Another ion pair [NH$_4^+$][BH$_3$NH$_2$BH$_3^-$] (**IonP-N**) could also exist as an alternative isomeric form of (**AB**)$_2$.

In the present work, we have carried out high-level electronic structure calculations to map out the relevant portions of the potential energy surface of the (**AB**)$_2$ dimer. Our goal is to probe further the molecular mechanism of the H$_2$ release from BNH$_6$ materials. We report the existence of a range of reaction pathways from the (**AB**)$_2$ dimer leading to H$_2$ production.

Computational Methods

Calculations were performed using the Gaussian 03[18] and MOLPRO 2002[19] suites of programs. Geometry parameters of the stationary points were initially optimized using second-order perturbation theory (MP2)[20] in conjunction with the correlation-consistent aug-cc-pVDZ basis set.[21] The character of each stationary point was subsequently determined to be an equilib-
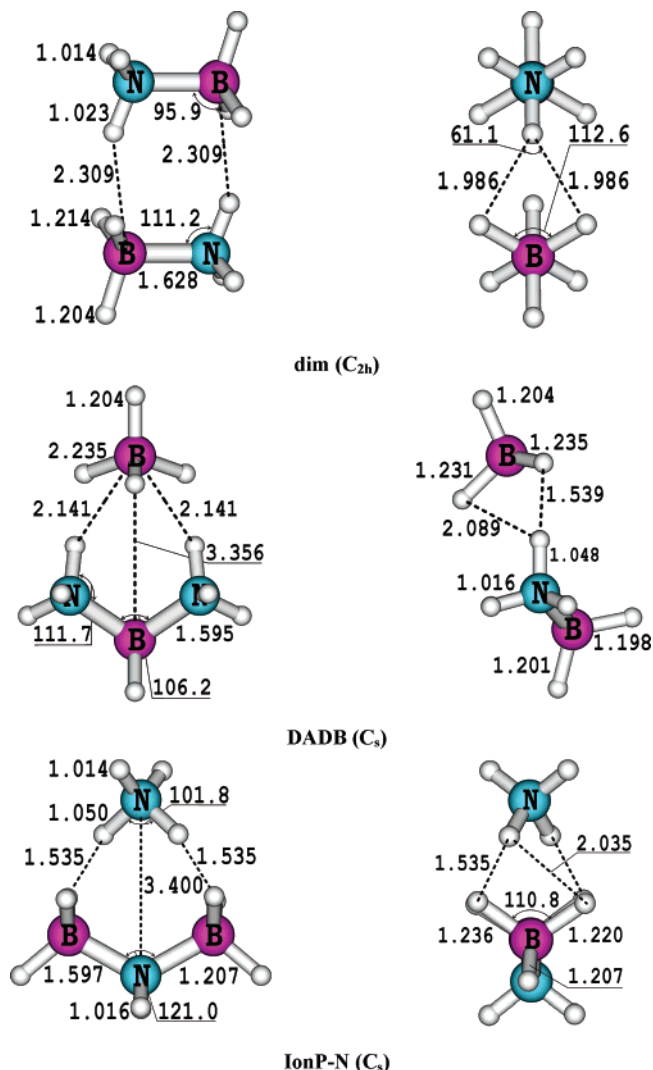

Figure 1. Selected MP2/aVTZ geometry parameters of the most stable ammonia borane dimer **dim** and its ion pair isomers **DADB** and **IonP-N**. Each structure is projected in two different plans. Bond lengths are given in Å, and bond angles in degrees.

TABLE 3: Calculated Heats of Formation at 0 and 298 K (kcal/mol) for B—N Compounds[a]

molecule	ΔH_f(0 K)	ΔH_f(298 K)
NH$_3$[b]	−9.6 ± 0.5	−11.3 ± 0.5
NH$_4^+$ [b]	153.6 ± 0.5	150.9 ± 0.7
BH$_3$[b]	26.4 ± 0.7	25.5 ± 0.7
BH$_4^-$ [b]	−11.6 ± 0.7	−13.5 ± 0.7
BH$_2$NH$_2$[b]	−15.9 ± 1.0	−18.6 ± 1.0
BH$_3$NH$_3$[b]	−9.1 ± 1.0	−13.5 ± 1.0
BH$_3$NH$_2$BH$_3^-$ [c]	−49.4 ± 1.2	−55.3 ± 1.2
NH$_3$BH$_2$NH$_3^+$ [c]	105.9 ± 1.2	99.2 ± 1.2
2(BH$_3$NH$_3$) (**dim**)[d]	−32.2 ± 1.0	−41.3 ± 1.0
BH$_3$NH$_2$BH$_2$NH$_3$ (**DADB-p1**)[d]	−27.4 ± 1.0	−35.3 ± 1.0
BH$_3$NH$_2$BH$_2$NH$_3$ (**DADB-p3**)[d]	−39.2 ± 1.0	−47.6 ± 1.0
NH$_3$BH$_2$NH$_3$···BH$_4$ (**DADB**)[c]	−21.6 ± 1.0	−31.0 ± 1.0
BH$_3$NH$_2$BH$_3$···NH$_4$ (**IonP-N**)[c]	−15.8 ± 1.0	−25.4 ± 1.0

[a] From CCSD(T)/CBS + correction calculations. [b] Reference 6. [c] This work. [d] Reference 42.

rium structure or a first-order saddle point, by second derivative calculations yielding harmonic vibrational frequencies at the same level. Harmonic vibrational frequencies were scaled to estimate the zero-point energies (ZPEs) based on previous analyses.[6,7,13] We used the accurate ZPE of BH$_3$NH$_3$[6] as a reference value to determine the scaling factor for (B$_x$N$_x$H$_y$)
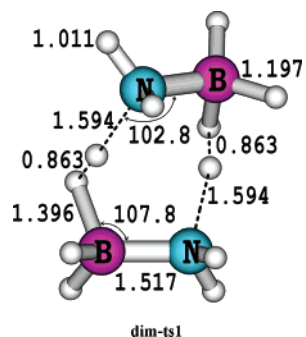
Figure 2. Selected MP2/aVTZ geometry parameters of the transition state structure **dim-ts1** for release of two H_2 molecules from **dim**. Bond lengths are given in Å, and bond angles in degrees.

derivatives. For MP2/aVDZ harmonic frequencies, a scaling factor of 0.9751 was obtained as the average of the MP2/aVDZ plus the accurate ZPE divided by the MP2/aVDZ value for BH_3-NH_3. To ascertain the identity of the relevant transition state (TS) structures, intrinsic reaction coordinate (IRC)[22] calculations were carried out using density functional theory with the hybrid B3LYP functional[23] and the 6-311++G(d,p) basis set. The IRC calculations were done with the default step size of 0.1 amu$^{1/2}$ bohr were calculated. Geometry parameters of the relevant structures were then refined at the MP2/aug-cc-pVTZ level.[21]

Improved relative energies between stationary points were calculated using coupled-cluster theory at the CCSD(T)[24] level using the MP2/aug-cc-pVTZ-optimized geometries. As a calibration for the variation of relative energies with respect to the basis set expansions, the CCSD(T) total energies of a few important structures were first extrapolated to the CBS limit, based on electronic energies obtained with the correlation-consistent aug-cc-pVnZ basis sets, with n = D, T, and Q. The extrapolation of the CCSD(T) energies to the CBS limit was done using the following expression[25]

$$E(n) = A_{CBS} + B \exp\left[-(n-1)\right] + C \exp\left[-(n-1)^2\right] \quad (1)$$

with n = 2, 3, and 4 for the aug-cc-pVnZ, n = D, T, and Q, basis sets, respectively (referred to hereafter as aVnZ). For the remaining structures, only CCSD(T)/aVTZ energies were considered. We have previously found that use of the aVTZ results will change the relative energies by less than 1 kcal/mol.[13,26] In the MP2 and CCSD(T) calculations, the core orbitals were kept frozen.

The lattice energy of the ionic salts was estimated using the volume approach proposed by Jenkins et al.[27] following previous work from the Bartlett group.[28] It is calculated from the empirical expression

$$U_L = 2I[\alpha V_m^{-1/3} + \beta] \quad (2)$$

where I is the ionic strength (I = 1 for MX (1:1) salts), and V_m is the molecular (formula unit) volume of the lattice involved, which is equal to the sum of the individual ion volumes of the cation, V_+, and anion, V_-. The electron densities were calculated using the B3LYP/DZVP2 level of density functional theory, and the volume corresponds to that inside the 0.001 au contour of the electron density. The choice of contour level was made on the basis of volumes used in free energy of solvation calculations.[29] For the empirical parameters in eq 2, the following values were used: α = 28.0 kcal/mol and β = 12.4 kcal/mol.[27] The lattice energies can be corrected to standard conditions at 298 K using eq 3[27]
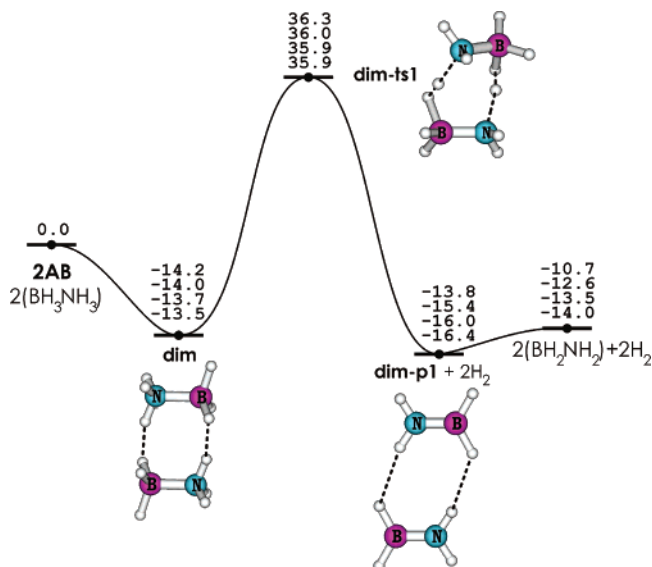

Figure 3. Schematic potential energy profiles, in kcal/mol, showing the reaction pathways for H_2 release from two ammonia borane monomers 2(BH_3NH_3) via the dimer **dim** and from **DADB**, calculated with the CCSD(T) method using four basis sets including ZPE corrections. The energies are from top to bottom: aVDZ, aVTZ, aVQZ, and CBS.
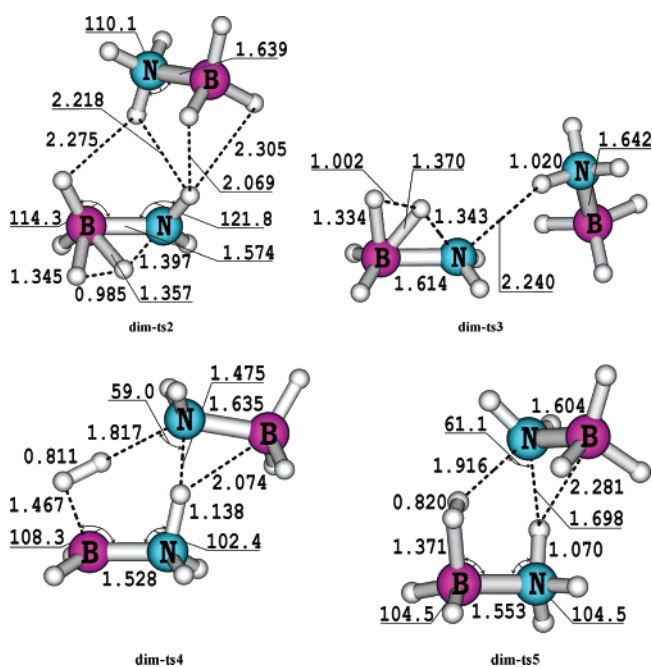

Figure 4. Selected MP2/aVTZ geometry parameters of four different TS's for release of one H_2 molecule from **dim**. Bond lengths are given in Å, and bond angles in degrees.

$$U_L(298\ K) = U_L + [p\ (n_M/2 - 2) + q\ (n_X/2)]RT \quad (3)$$

for M_pX_q salts, where $n_M = n_X = 6$ for nonlinear polyatomic ions.

Results and Discussion

Stability of Ammonia Borane Dimer and Its Ion Pair Isomers. The calculated relative energies of the three isomeric structures are listed in Table 1. The complexation energy of the dimer with respect to the two **AB** monomers, chosen as the energy reference, is summarized in Table 2. Total CCSD(T)
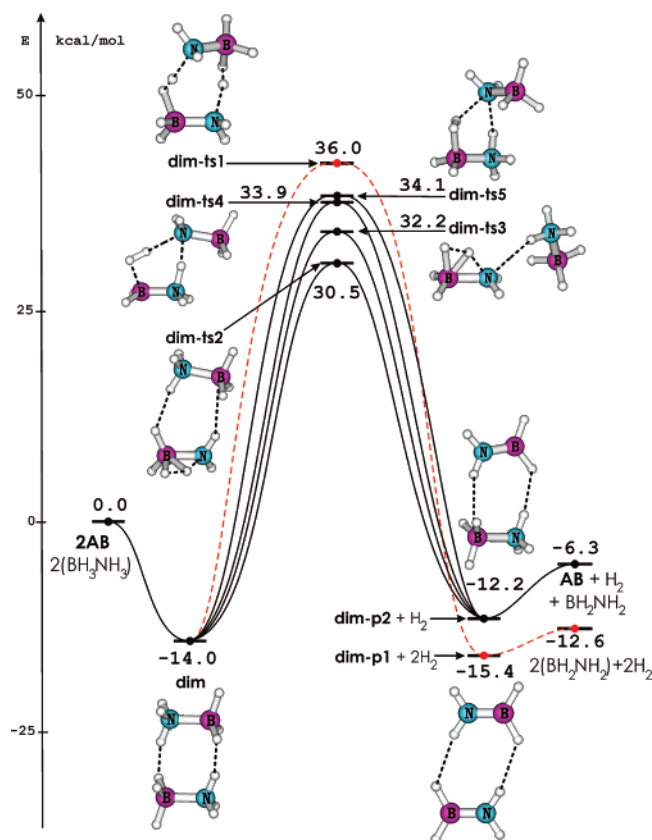
Figure 5. Schematic potential energy profiles illustrating five different reaction pathways for H$_2$ release from the ammonia borane dimer **dim.** Relative energies given in kcal/mol were obtained from CCSD(T)/aVTZ + ZPE calculations.

and ZPEs for the isomers and the NH$_3$BH$_2$NH$_3^+$ and BH$_3$NH$_2$BH$_3^-$ ions are tabulated in Table S-1 of the Supporting Information.

The geometry and complexation energy of the (**AB**)$_2$ dimer has previously been investigated.[30–42] The nature of the hydrogen-bond interaction in the dimer has been the subject of most of these analyses. Our present calculations confirm that the dimer has a number of low-energy conformations with different symmetry point groups. The energy differences between these different conformations are very small, less than 0.5 kcal/mol. The structure characterized by C_{2h} symmetry and denoted hereafter as **dim**, is the energetically lowest-lying dimer conformation that we found. One N—H bond of an **AB** monomer interacts with two B—H bonds of the other monomer. Selected optimized geometry parameters at the MP2/aVTZ level are displayed in Figure 1. The H(N)···H(B) intermolecular distance of 1.986 Å in **dim,** optimized at MP2/aVTZ level, differs from the values optimized at lower levels.[30–34] The B—H and N—H bond distances within the B—H···H—N dihydrogen bond are longer than the non-interacting ones by up to 0.01 Å. The atomic net charges (q) of the four B—H···H—N atoms are: $q(B) = 0.42e$, $q(H) = -0.33e$, $q(H) = 0.20e$, and $q(N) = 0.17e$ at the HF/aVTZ level, corresponding to a B—H$^{\delta-}$···H—N$^{\delta+}$ charge distribution consistent with the analysis of Li et al.[37] These authors suggested in addition that the main factor of the hydrogen bond is a charge transfer from the occupied σ(B—H) orbital to the vacant σ^*(X—H) orbitals.[37]

We have previously calculated the heat of formation of **dim** $\Delta H_f[(BH_3NH_3)_2]$ to be -32.2 kcal/mol at 0 K and -41.3 kcal/mol at 298 K.[42] As in the **AB** monomer case,[6] the error bar from the total atomization energies using CCSD(T)/CBS energies and other corrections is expected to be ± 1.0 kcal/mol for the heat of formation of the dimer. In conjunction with the

previously calculated heats of formation of the **AB** monomer[6] $\Delta H_f(BH_3NH_3) = -9.1 \pm 1.0$ kcal/mol at 0 K and $\Delta H_f(BH_3\text{-}NH_3) = -13.5 \pm 1.0$ kcal/mol at 298 K, the complexation energy of **dim** is -14.0 kcal/mol at 0 K and -14.3 kcal/mol at 298 K. Previous B3LYP[31] and MP2[37] calculations predicted a complexation energy of about -11 kcal/mol for **dim**. As shown in Table 2, the complexation energy of **dim** is calculated to be -14.0, -13.7, and -13.5 kcal/mol using the CCSD(T) method with the aVTZ, aVQZ, and estimated CBS basis sets, respectively, including ZPE corrections. The result of -13.5 kcal/mol at the CCSD(T)/CBS + ZPE level differs by 0.5 kcal/mol from that of -14.0 kcal/mol obtained previously[42] This difference arises from the core—valence correlation and scalar relativistic corrections that were included in the previous work. Our current aVTZ value of -14.0 kcal/mol for the complexation energy of the dimer **dim** is thus in good agreement with the previous higher-level calculations.[42]

Two isomers of **dim** with ion pair structures were also located. Selected MP2/aVTZ geometry parameters are also given in Figure 1. **DADB** contains a [BH$_4^-$] anion whereas **IonP-N** bears a [NH$_4^+$] cation. Both isomers exhibit C_s symmetry with the B—H and N—H bonds interacting strongly with each other. In **DADB**, the interior (B)H—H(N) distance of 1.539 Å is relatively short, much shorter than the H···H distance of 1.986 Å in neutral **dim**. Similarly, the interior (N)H—H(B) distance in **IonP-N** is 1.535 Å. These geometric results show strong ionic interactions between the anion and the cation in the ion pairs.
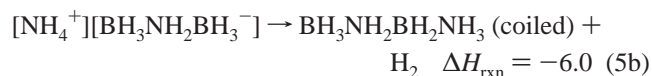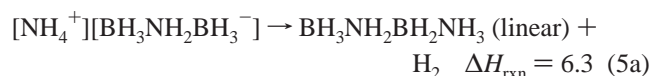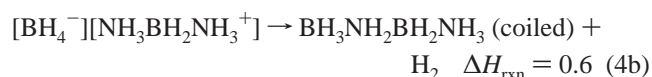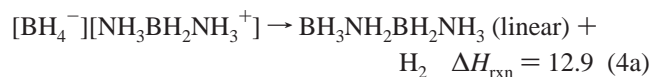
We calculated the heats of formation of both ion pairs in the gas phase by using the total atomization energies computed at the CCSD(T)/CBS level plus additional corrections for the ZPE, core—valence effects,[43] scalar relativistic effects,[44] and atomic spin orbit effects[45] following our prior work.[6,7,13] The raw data for the atomization energies are given in Table S-2 of the Supporting Information. The atomization energy was converted to a heat of formation by using the 0 K atomic heats of formation of $\Delta H_f^\circ(N) = 112.53 \pm 0.02$ kcal mol^{-1}, $\Delta H_f^\circ(B) = 136.2 \pm 0.2$ kcal mol^{-1}, and $\Delta H_f^\circ(H) = 51.63 \pm 0.001$ kcal mol^{-1}.[46,47] Heats of formation at 298 K were obtained following the procedure of Curtiss et al.[48] We obtain $\Delta H_f[\textbf{DADB}] = -21.6$ and -31.0 kcal/mol at 0 and 298 K, respectively, and $\Delta H_f[\textbf{IonP-N}] = -15.8$ and -25.4 kcal/mol at 0 and 298 K. Accordingly, the **DADB** ion pair is found to be 10.6 kcal/mol less stable than **dim**. The **IonP-N** ion pair is even less stable, 16.4 kcal/mol above **dim.** We compile in Table 3 our calculated values at both 0 and 298 K, together with other relevant literature results.[6,42]

In the solid state, the ion pairs are expected to exist as ionic salts, and the lattice energies resulting from the salts could stabilize them differently. The corresponding volume for the salt [BH$_4^-$][NH$_3$BH$_2$NH$_3^+$] is $V_m = 0.1452$ nm^3 obtained from the sum of the cation, $V_+(\text{NH}_3\text{BH}_2\text{NH}_3^+) = 0.0792$ nm^3, and the anion, $V_-(\text{BH}_4^-) = 0.066$ nm^3. The lattice energy of the crystal salt from Coulombic interaction between both [BH$_4^-$] and [NH$_3$BH$_2$NH$_3^+$] ions is calculated to be 131.5 kcal/mol at 0 K, using eq 2, and 133.9 kcal/mol at 298 K, using eq 3. The heats of formation of the ions in the gas phase are $\Delta H_{0K}(\text{BH}_4^-) = -11.6$ kcal/mol, $\Delta H_{298K}(\text{BH}_4^-) = -13.5$ kcal/mol,[6] $\Delta H_{0K}(\text{NH}_3\text{-}\text{BH}_2\text{NH}_3^+) = 105.9$ kcal/mol, and $\Delta H_{298K}(\text{NH}_3\text{BH}_2\text{NH}_3^+) = 99.2$ kcal/mol. The heat of formation of NH$_3$BH$_2$NH$_3^+$ was calculated from total atomization energies at the CCSD(T)/CBS level with the additional corrections described above. The zero-point corrections were obtained from MP2/aVTZ harmonic vibrational frequencies and scaled by a factor of 0.9684 obtained as described above. The various components are given in Table

S-2 of the Supporting Information. From a Born–Haber cycle, the heat of formation of the salt, $[BH_4^-][NH_3BH_2NH_3^+]$, is predicted to be -37.2 kcal/mol at 0 K and -48.2 kcal/mol at 298 K with an estimated error of ± 5 kcal/mol due mostly to the simple model for the solid-state energy. The gas-phase binding energy of the ion pair from the heats of formation is 116.9 kcal/mol at 0 K, showing that all but ~ 15 kcal/mol of the lattice energy is due to the interaction of a single ion pair.

For the second salt, $[NH_4^+][BH_3NH_2BH_3^-]$, the corresponding volume is $V_m = 0.1324$ nm^3 obtained from the sum of the cation, $V_+(NH_4^+) = 0.0210$ nm^3, and the anion, $V_-(BH_3NH_2BH_3^-)$ $= 0.1114$ nm^3. The lattice energy is calculated to be 134.8 kcal/mol at 0 K and 137.2 kcal/mol at 298 K. The heats of formation of the ions in the gas phase are $\Delta H_{0K}(NH_4^+) = 153.6$ kcal/mol, $\Delta H_{298K}(NH_4^+) = 150.9$ kcal/mol,[6] $\Delta H_{0K}(BH_3NH_2BH_3^-)$ $= -49.4$ kcal/mol, and $\Delta H_{298K}(BH_3NH_2BH_3^-) = -55.3$ kcal/mol. The heat of formation of $BH_3NH_2BH_3^-$ was calculated from total atomization energies at the CCSD(T)/CBS level with the additional corrections described above. The various components are given in Table S-2 of the Supporting Information. The heat of formation of the salt, $[NH_4^+][BH_3NH_2BH_3^-]$, is estimated to be -30.7 kcal/mol at 0 K and -41.6 kcal/mol at 298 K with an estimated error of ± 5 kcal/mol. The difference in the heats of formation of the salts at 0 K is 6.5 kcal/mol favoring $[BH_4^-][NH_3BH_2NH_3^+]$, very similar to the difference of 5.8 kcal/mol for the gas-phase ion pairs. The ionic binding energy in the gas phase between the two ions is 120.0 kcal/mol at 0 K, and, again, all but ~ 15 kcal/mol of the lattice energy is due to the interaction of a single ion pair.

From the gas-phase heats of formation of $BH_3NH_2BH_2NH_3$, linear trans and coiled (gauche) structures,[42] we can calculate the following H_2 elimination energies from the salts in kcal/mol at 298 K

$$[BH_4^-][NH_3BH_2NH_3^+] \rightarrow BH_3NH_2BH_2NH_3 \text{ (linear)} +$$
$$H_2 \quad \Delta H_{rxn} = 12.9 \quad (4a)$$

$$[BH_4^-][NH_3BH_2NH_3^+] \rightarrow BH_3NH_2BH_2NH_3 \text{ (coiled)} +$$
$$H_2 \quad \Delta H_{rxn} = 0.6 \quad (4b)$$

$$[NH_4^+][BH_3NH_2BH_3^-] \rightarrow BH_3NH_2BH_2NH_3 \text{ (linear)} +$$
$$H_2 \quad \Delta H_{rxn} = 6.3 \quad (5a)$$

$$[NH_4^+][BH_3NH_2BH_3^-] \rightarrow BH_3NH_2BH_2NH_3 \text{ (coiled)} +$$
$$H_2 \quad \Delta H_{rxn} = -6.0 \quad (5b)$$

The reaction 5b giving the stable coiled structure is exothermic, whereas formation of the linear structure is endothermic. Reaction 4b is very close to thermoneutral.

Reaction Pathways For H_2 Release from Ammonia Borane Dimer. We first consider the energy barriers for the production of H_2 molecules from **dim**. Geometries of the relevant TS's are displayed in Figures 2 and 4, and the potential energy diagrams constructed at the CCSD(T) level with different basis sets are illustrated in Figures 3 and 5. Results for the relative energy of some important structures as a function of basis sets are given in Table 2, whereas relative energies obtained with both aVDZ and aVTZ basis sets are listed in Table 4. Total energies, ZPEs, and Cartesian coordinates of all of the optimized structures are listed in Tables S-3 and S-4 of the Supporting Information. Geometry parameters of three additional TS's denoted as **dim-ts6**, **dim-ts7**, and **dim-ts8** for H_2 release from **dim** were also optimized and shown in Figure S-1 of the

TABLE 4: CCSD(T) Relative Energies Including ZPE Corrections (kcal/mol) of Equilibrium and Transition State Structures for H_2 Release from Ammonia Borane Dimer[a]

structures	aVDZ	aVTZ
2AB	0.0	0.0
dim	-14.2	-14.0
dim-ts1	36.3	36.0
dim-ts2	31.2	30.5
dim-ts3	32.8	32.2
dim-ts4	34.3	33.9
dim-ts5	34.9	34.1
dim-p1 $+ 2H_2$	-13.8	-15.4
$2(BH_2NH_2) + 2H_2$	-10.7	-12.6
dim-p2 $+ H_2$	-11.5	-12.2
AB $+ BH_2NH_2 + H_2$	-5.4	-6.3

[a] Calculated at the CCSD(T) level using MP2/aVTZ-optimized geometries and scaled MP2/aVDZ ZPE corrections.

Supporting Information. These TS's are however located at much higher energies and therefore not discussed further in the following section.

dim-ts1 is the TS for generating two H_2 molecules with each monomer contributing one H_2 molecule (Figure 2). Formation of each H_2 occurs within a B–H···H–N **dim** framework, involving a short H–H distance of 0.863 Å, close to the bond distance of 0.74 Å in H_2. The reaction proceeds by an eight-membered ring TS. The N–H distance of 1.594 Å is proportionally more stretched than the B–H bond (1.396 Å). The B–H and N–H bonds distances of 1.197 and 1.011 Å in the molecule are shorter than that of the B–H···H–N dihydrogen bond. A high barrier of 49.4 kcal/mol is found (Figure 3, CCSD-(T)/CBS values). The two aminoborane molecules (BH_2NH_2) also form a weak complex **dim-p1** in the exit channel with a complexation energy of -2.4 kcal/mol. The product $2(BH_2NH_2)$ $+ 2H_2$ lies 0.5 kcal/mol below **dim**, which is close to a thermoneutral reaction.

As shown in Table 2, the energy barriers converge quickly with respect to the basis set. The values obtained at the CCSD-(T)/aVTZ and CCSD(T)/aVQZ levels for **dim** differ only by, at most, 0.5 and 0.2 kcal/mol, respectively, from the CCSD-(T)/CBS counterparts. This is consistent with what we have found previously.[13,26] These results show that use of the computationally less-demanding CCSD(T)/aVTZ level can be used to construct the potential energy surfaces for these systems, with an expected accuracy of ± 1.0 kcal/mol for the energy barriers as compared to the CBS limit.

In addition to the **dim-ts1** described above, we located four other TS's for release of one H_2 molecule from **dim**. Figure 4 shows critical MP2/aVTZ geometry parameters of these TS's, and Figure 5 summarizes the reaction pathway energetics.

dim-ts2 is basically an H_2 elimination from one **AB** monomer[13] with a TS that is complexed with the second monomer by H–H interactions from the side opposite to the departing H_2. The intermolecular H–H distances range from 2.069 to 2.305 Å, and a B–H···H–N skeleton is present with bond distances of 1.211, 2.069, and 1.011 Å, respectively. The energy for this TS is 30.5 kcal/mol above the separated monomers and 44.5 kcal/mol above the dimer **dim** (values at the CCSD(T)/aVTZ + ZPE level, Figure 5). The product **dim-p2** is characterized as a hydrogen-bonded complex between BH_3NH_3 and BH_2NH_2, with a complexation energy of -5.9 kcal/mol. The product **dim-p2** $+ H_2$ is calculated to be 1.8 kcal/mol above **dim**.

dim-ts3 corresponds to a comparable process to that involving **dim-ts2**, but the intermolecular interaction mainly involves a type of N···H–N hydrogen bond. The N–H bond of the
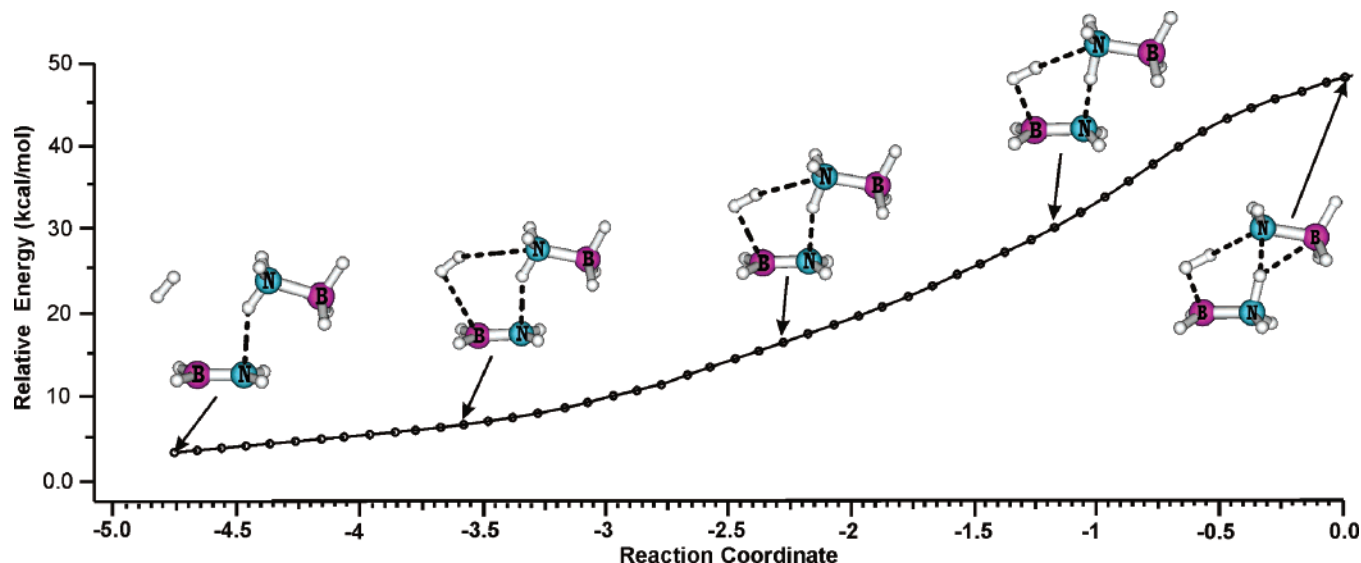
Release of H$_2$ from (BH$_3$NH$_3$)$_2$

J. Phys. Chem. A, Vol. 111, No. 36, 2007 **8849**

Figure 6. An IRC pathway showing the formation of the product **dim-p2** from **dim-ts4**, calculated using the B3LYP/6-311++G(d,p) level. IRC calculations starting from the TS were done with the default step size of 0.1 amu$^{1/2}$ bohr.

nonreacting monomer plays the role of the hydrogen-bond donor, with an intermolecular N···H distance of 2.240 Å. Parameters within the four-membered cycles involving the forming H$_2$ in both **dim-ts2** and **dim-ts3** differ somewhat from each other, with B—N distances varying up to 0.04 Å. The role of the second monomer is described in more detail below. The energy of **dim-ts3** is higher, by 1.7 kcal/mol, than **dim-ts2**. The process through **dim-ts3** also gives rise to the same product **dim-p2**.

The reaction path proceeding through **dim-ts4** shows another way of eliminating H$_2$. The departing H$_2$ is composed of one H(B) atom of the first monomer plus one H(N) atom of the second monomer. The strongest intermolecular interaction arises from a N—H···N hydrogen bond involving quite short N—H distances of 1.138 and 1.475 Å, so the H is partially transferred. In **dim-ts4**, both BH$_3$ groups are trans with respect to the N—H···N bond. The B—N—H···N—B frame lies almost in the same plane. The H—H distance of 0.811 Å shows that the product H$_2$ molecule is almost completely formed. **dim-ts4** is close to the TS for H$_2$ release from BH$_3$NH$_3$ assisted by a NH$_3$ molecule that we previously reported.[13] In this case, the second monomer plays the role of the bifunctional catalyst. The channel involving **dim-ts4** has energy barriers of 33.9 and 47.9 kcal/mol with respect to two **AB** monomers and **dim**, respectively, to produce one H$_2$. **dim-ts4** is 1.7 kcal/mol higher in energy than **dim-ts3** and could lead to the chain product **DADB-p1** (BH$_3$NH$_2$BH$_2$-NH$_3$) involved in reactions 4 and 5. Upon loss of H$_2$, both tri-coordinated B and N atoms could join to make a new B—N bond. However, extensive IRC calculations demonstrate that an H transfer between two N atoms takes place yielding the complex **dim-p2**. The corresponding IRC path for product formation from **dim-ts4** at the B3LYP/6-311++G(d,p) level is displayed as Figure 6.

dim-ts5 involves a similar kind of process to that proceeding through **dim-ts4** with the main difference between **dim-ts4** and **dim-ts5** being that in the latter the BH$_3$(N) group of the second monomer is nearly perpendicular to the B—N—N plane. The intermolecular distances in **dim-ts5** are markedly longer than those in **dim-ts4**. **dim-ts5** corresponds to the energetically highest-lying TS among the four TS's examined. It still is only 3.6 kcal/mol above **dim-ts2**. Again, **dim-ts5** leads to the product **dim-p2**.

The energy profiles summarized in Figure 5 show that the energies of the five TS's do not differ substantially from each other. The difference between the lowest-lying **dim-ts2** and the highest-lying **dim-ts1** is 5.5 kcal/mol. The catalytic effect of simple dihydrogen-bonded interactions via **dim-ts2** and **dim-ts3** is slightly more effective than the bifunctional hydrogen exchange via **dim-ts4** and **dim-ts5**. Nevertheless, the smallest barrier is 44.5 kcal/mol above the dimer **dim**. This is much larger than the dimerization energy of **AB** of only 14.0 kcal/mol (values at CCSD(T)/aVTZ + ZPE) and is above the dimerization energy plus breaking one **AB** B—N bond. Thus, the dimer **dim** is expected to undergo dissociation rather than H$_2$ production under mild thermal conditions.

Formation of the Diammoniate of Diborane Ion Pair (DADB) and H$_2$ Release from Two Ammonia Borane Molecules. We now consider the formation of **DADB** from three distinct starting points: 2BH$_3$NH$_3$, B$_2$H$_6$ + 2NH$_3$, and BH$_3$-NH$_3$ + NH$_3$ + BH$_3$. Selected geometry parameters of all related structures are given in Figure 7. These include four TS's for the formation of **DADB** (Figure 7a), three complexes formed from BH$_3$HBH$_2$NH$_3$ + NH$_3$, with different orientations of the NH$_3$ (Figure 7b), and also three TS's for H$_2$ release from intermediates (Figure 7c). Figure 8 schematically illustrates the reaction pathways leading to **DADB** formation and to H$_2$ formation.

As shown in Figure 8, all three reactant systems **2AB**, B$_2$H$_6$ + 2NH$_3$ (denoted as **DB** + 2A), and BH$_3$NH$_3$ + NH$_3$ + BH$_3$ (denoted as **AB** + A + B) undergo additions and rearrangements converging to the same adduct **BBA-com** + A in the first step. **BBA-com** is a key common intermediate in these processes and is the adduct of **AB** with BH$_3$, which was studied in detail in our previous paper.[13] Thus, condensation of **AB** + A + B invariably leads to **BBA-com** + B without an activation energy barrier.

BBA-com + B is calculated to be 8.1 kcal/mol above the two separated monomers **2AB** and substantially below **AB** + B + A. Addition from **2AB** involves an energy barrier of 12.4 kcal/mol via TS **2AB-ts1**. The TS involves the attack of the B atom in one **AB** on an H atom of the BH$_3$ in another **AB**. Formation of a bridge B—H—B bond induces breakage of the N—B bond in the attacking **AB** to eliminate NH$_3$. The BH distances of 1.700 and 1.229 Å in **2AB-ts1** show a forming
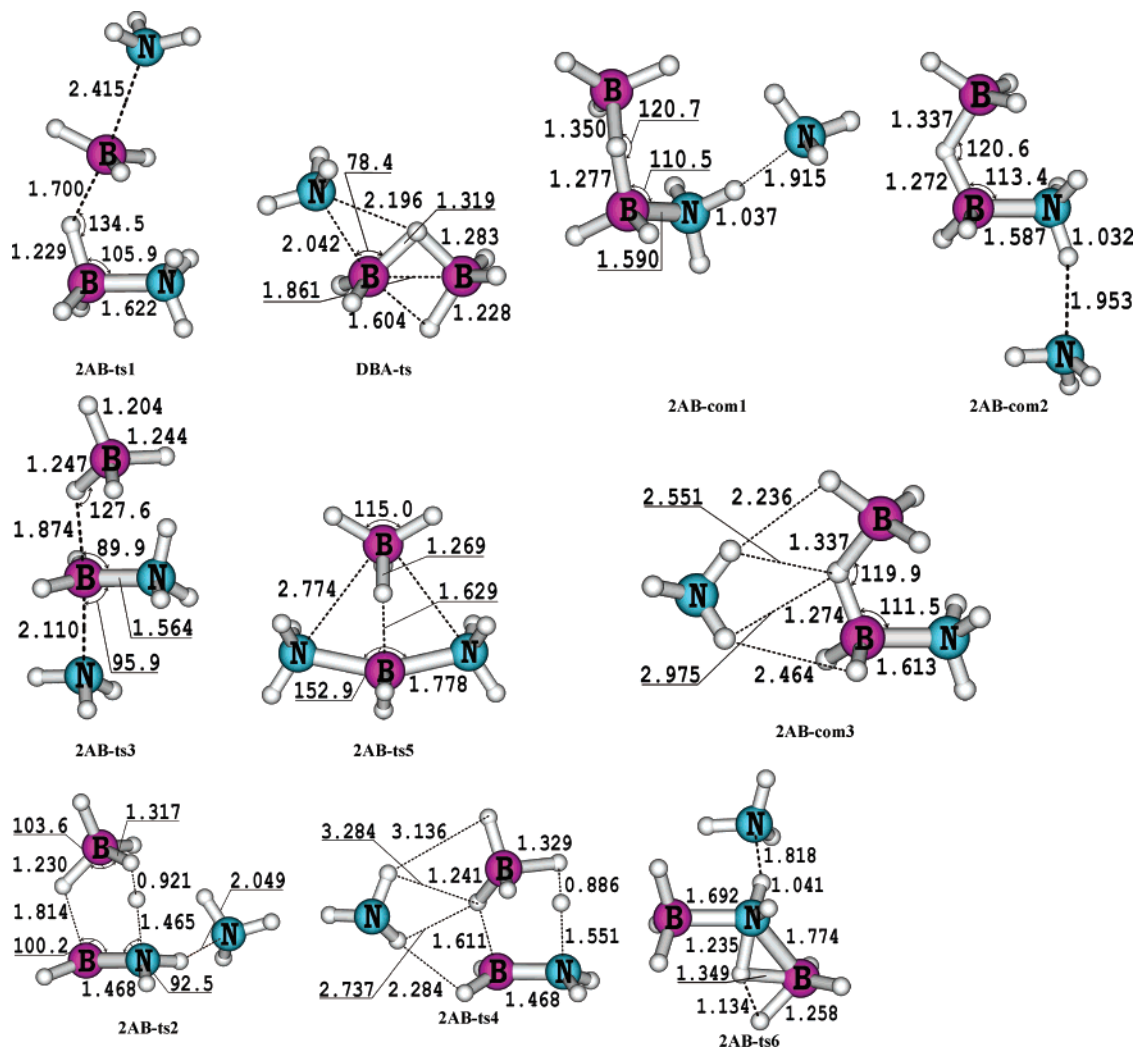
Figure 7. Selected MP2/aVTZ geometry parameters of four different TS's for formation of **DADB** from **2AB**, **DB** + 2A, and **AB** + A + B. Selected MP2/aVTZ geometry parameters of three different complexes for formation of **DADB** from **2AB**, **DB** + 2A, and **AB** + A + B. Selected MP2/aVTZ geometry parameters of three different TS's for H₂ release from **2AB**, **DB** + 2A, and **AB** + A + B. Bond lengths are given in Å, and bond angles in degrees.

B—H—B bond. The stretching of the N—B bond in the second **AB** by ~0.8 Å to 2.415 Å is consistent with breaking a B—N bond (cf. Figure 7a).

The barrier-free condensation of diborane (**DB**) with one NH₃ molecule forms the complex **DBA-com**, which has a complexation energy of −5.1 kcal/mol and is 12.6 kcal/mol above **2AB**. This weak complex is characterized by long distances between N and a bridge BH bond (not shown in Figure 7b). Conversion of **DBA-com** to **BBA-com** occurs with an energy barrier of 7.8 kcal/mol through TS **DBA-ts,** which lies 20.4 kcal/mol above **2AB**. **DBA-ts** is formed by a nearly perpendicular attack of N of a free NH₃ to a B center of **DB** (∠NBH angle = 78.4° and N—B = 2.042 Å). When NH₃ approaches the diborane plane defined by BH$_b$BH$_b$, the attack on one B—H—B bond induces breaking of the other B—H—B bond. The broken B—H distance is 1.604 Å in **DBA-ts** (Figure 7a). The identity of both TS's was confirmed by IRC calculations at the B3LYP level with the 6-311++G(d,p) basis set.[49]

At this point, we have described the formation of **BBA-com** + A as separated species that represent another asymptotic region. This asymptote provides a common entry point to an interesting region of the potential energy surface. When **BBA-com** and A are allowed to interact, they exothermically form without a barrier a variety of hydrogen-bonded complexes depending on the orientation of the NH₃. Figure 7 shows three

complexes **2AB-com1**, **2AB-com2**, and **2AB-com3** with different formation energies and related to **DADB** or H₂ formation. Of these complexes, **2AB-com1** is located at the lowest-energy position, 1.0 kcal/mol below **2AB**, and has an intermolecular N—H bond between the N of the free NH₃ and an H of the NH₃ in **BBA-com**. **2AB-com1** is characterized by the largest complexation energy of −9.1 kcal/mol with respect to **BBA-com** + A. The small energy difference between **2AB** and **2AB-com1** means that the energy lost by breaking the B—N bond in an **AB** monomer is fully recovered by the new B—H—B and N—H—N bonds in the complex.

2AB-com2 is a slightly weaker complex, formed by the same type of N—H—N interaction as in **2AB-com1,** but with a different of NH₃ orientation. In this case, the NH₃ is connected to one H atom of the bonded NH₃ group and is in a trans position with respect to the BH₃ of **BBA-com** complexed to the H from the BH₃NH₃ moiety. **2AB-com2** is only 0.7 kcal/mol less stable than **2AB-com1** and is 0.3 kcal/mol below **2AB**. There is a spectrum of complexes between **BBA-com** and NH₃ that differ from each other by rotation of the NH₃. These are however less stable than the two complexes just discussed.

2AB-com3 has four N—H—H—B interactions between the N—H bonds of the free NH₃ and B—H bonds belonging to **BBA-com.** The H—H bond distances are long, ~3.0 Å, and the complex is weak with a complexation energy of only −1.1 kcal/
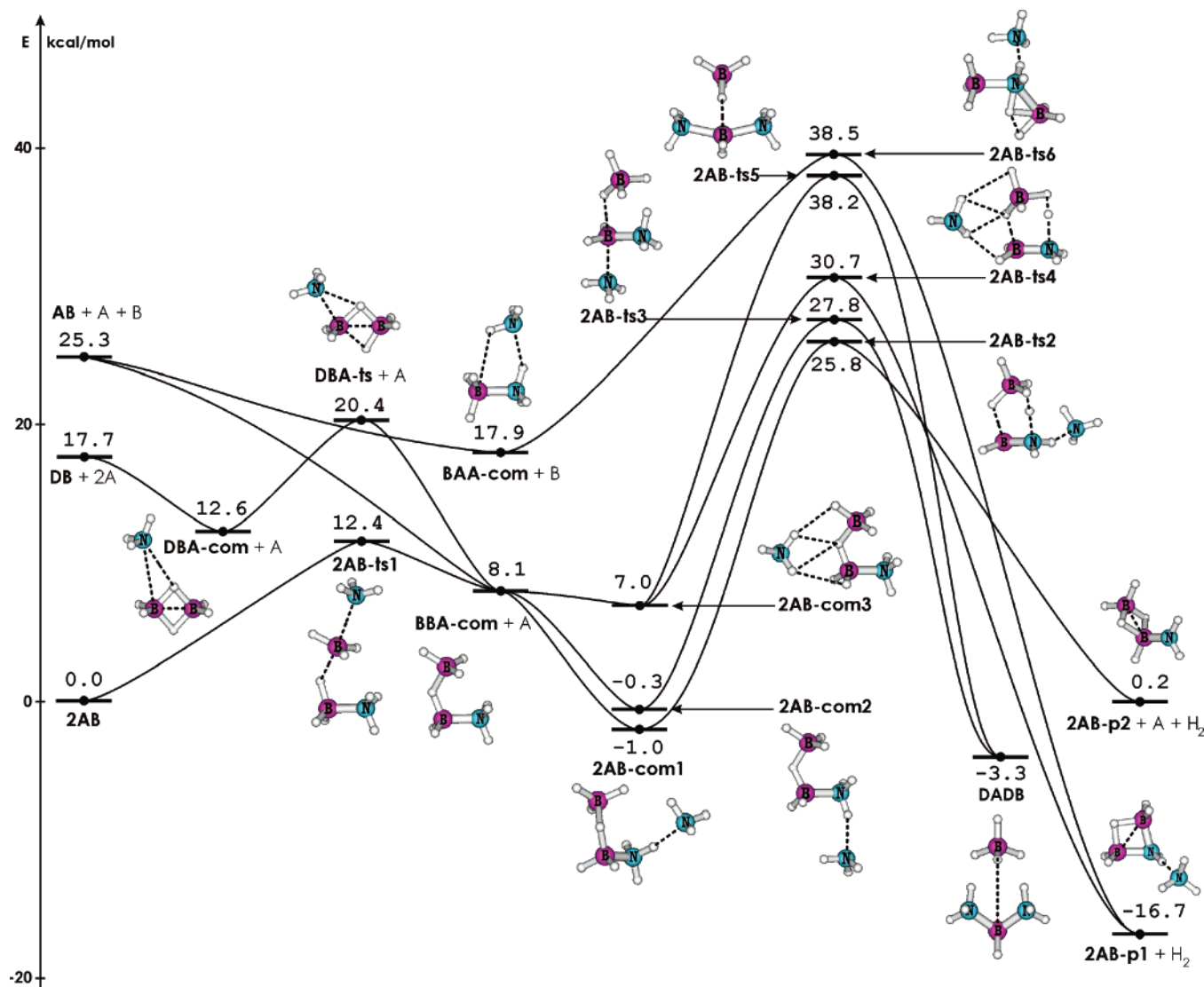
Figure 8. Schematic energy profiles illustrating the different reaction pathways for formation of **DADB** from **2AB**, **DB** + 2A, and **AB** + A + B. Relative energies given in kcal/mol were obtained from CCSD(T)/aVTZ + ZPE calculations.

mol with respect to separated **BBA-com** + A fragments. **2AB-com3** is 7.0 kcal/mol above **2AB** and 8.0 kcal/mol above **2AB-com1**.

As shown in Figure 8, **DADB** can be formed from unimolecular rearrangements of **2AB-com2** and **2AB-com3** but not from **2AB-com1**. **2AB-com2** is connected to **DADB** by an energy barrier of 28.1 kcal/mol via TS **2AB-ts3.** This is the sole TS from **2AB-com2** and is located at 27.8 kcal/mol above **2AB**. Conversion of **2AB-com3** to **DADB** has a larger energy barrier of 31.2 kcal/mol through TS **2AB-ts5** (38.2 kcal/mol above **2AB**). Geometries of these TS's are shown in Figure 7.

DADB can also be formed from **2AB-com3** by overcoming an energy barrier of 31.2 kcal/mol at TS **2AB-ts5** (38.2 kcal/mol above **2AB**). The higher energy of the latter TS, relative to **2AB-ts3**, is due to different factors. A simultaneous breaking of not only the bridged B—H—B but also four N—H—H—B bonds, even though they are weak, occurs. In **2AB-ts5**, the new BN and BH bonds and, thus, both cationic and anionic moieties have essentially been formed. Such a "late" transition state is usually associated with a higher barrier. However, formation of **DADB** is not the favored rearrangement of **2AB-com3**. Indeed it undergoes preferentially loss of H$_2$ with a lower-energy barrier of 23.7 kcal/mol via TS **2AB-ts4** (Figure 7, 30.7 kcal/

mol above **2AB**), producing cyclic **2AB-p1**. The latter TS **2AB-ts4** is basically composed of the TS for H$_2$ loss from **BBA-com**, reported in our previous paper,[13] with complexation by an additional NH$_3$. A difference of 7.5 kcal/mol between the energies of both TS's clearly points out the dominance of the H$_2$ elimination over **DADB** formation from **2AB-com3**.

We also found another pathway for H$_2$ release from **2AB-com1** via TS **2AB-ts2** in which one H$_2$ can be generated by the same mechanism as in **BBA-com**[13] and again complexed by NH$_3$ but on the amine side. This TS is close to **2AB-ts4**, but they differ from each other by the position of the NH$_3$ and different hydrogen-bond interactions. **2AB-ts2** is lower in energy than **2AB-ts4** by 4.9 kcal/mol; it is 25.8 and 26.8 kcal/mol above **2AB** and **2AB-com1**, respectively. In this case, the products **2AB-p2** + NH3 + H$_2$ are only 0.2 kcal/mol above **2AB**.

From the **AB** + A + B asymptote, the interaction between **AB** and NH$_3$ leads directly to the complex **BAA-com**, which was also studied in our previous study.[13] **BAA-com** is characterized by an N—H hydrogen-bond distance of 1.99 Å, and additional stability is provided by a weaker B—H—N interaction. (The B—H(NH$_3$) bond is 2.68 Å.) In this complex, NH$_3$ plays the role of a hydrogen-bond acceptor, and **AB** is a hydrogen-bond donor. The energy of **BAA-com** + BH$_3$ is 17.9 kcal/mol
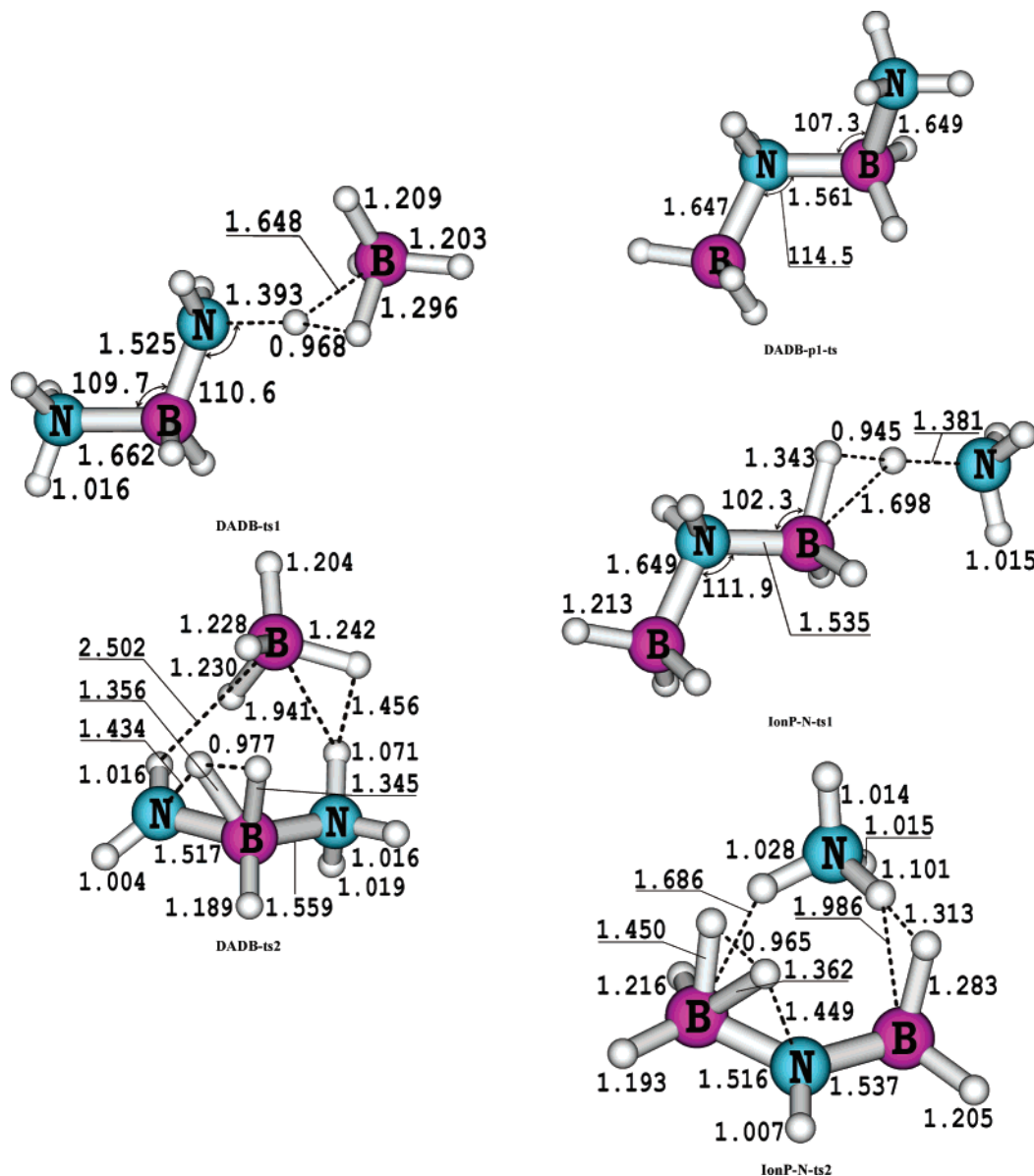
Figure 9. Selected MP2/aVTZ geometry parameters of five different TS's for H_2 release from **DADB** and **IonP-N**. Bond lengths are given in Å, and bond angles in degrees.

above **2AB** and 7.4 kcal/mol below **AB** + A + B. With the assistance of BH_3, one H_2 molecule can be generated from **BAA-com** + B through TS **2AB-ts6** (Figure 7c) with an energy barrier of 20.6 kcal/mol (**2AB-ts6** is 38.5 kcal/mol above **2AB**). This TS results from an attack of the B of free BH_3 to the N of NH_3 in **BAA-com**, and the two departing H atoms are bonded at a distance of 1.134 Å. One H atom is released from NH_3 in **BBA-com** and the other from free BH_3. IRC calculations showed that the products of this TS are also **2AB-p1** + A + H_2 (as from **2AB-com3**). **2AB-ts6** corresponds to a TS for H_2 loss of a **AB** monomer interacting simultaneously with BH_3 and NH_3. As shown in Figure 8, the reaction pathway involving **BAA-com** + B is less favored with respect to the paths discussed above. **2AB-ts6** represents the highest-lying saddle point in this region of the potential energy surface.

In summary, the results in Figure 8 show that a reaction starting from two monomers **2AB** yields the complexes **2AB-com1** and **2AB-com2** as reactive intermediates. The complexes undergo subsequent H_2 release and **DADB** formation reactions characterized by energy barriers of 25.8 kcal/mol via **2AB-ts2** and 27.8 kcal/mol via **2AB-ts3**, respectively. An energy

difference of 2 kcal/mol between both TS's is small and close to the expected accuracy of our calculations at the CCSD(T)/aVTZ + ZPE level. Other factors besides the simple barrier heights could play a role in the kinetics. Thus both channels, H_2 release and **DADB** formation, should be competitive. Although energetically less favored, the **BAA-com** + B and **2AB-com3** systems also connect other regions of the potential energy surface, such as the channel giving rise to diborane (B_2H_6) as a product. We have recently probed the reaction of diborane with ammonia, which follows similar reaction pathways.[26,49]

We now address the role of the second **AB** monomer in the various transformations. We showed[13] that B—N bond cleavage is favored by ~10 kcal/mol over an H_2 loss from one **AB** monomer. The role of the second monomer is to provide the BH_3 and NH_3 that can catalyze loss of H_2 from the remaining monomer or to assist in forming various complexes associated with breaking a B—N bond. The reaction pathways related to the **2AB** and **AB** + A + B systems given in Figure 8 show that the **AB** monomer can assist in breaking the B—N bond as

TABLE 5: CCSD(T) Relative Energies (kcal/mol) of Transition State and Equilibrium Structures for Formation DADB and H_2 Release from the 2AB, DB + 2A, and AB + A + B[a]

structures	aVDZ	aVTZ
2AB	0.0	0.0
DB + 2A	17.9	17.7
AB + A + B	24.0	25.3
DBA-com + A	12.2	12.6
BAA-com + B	16.5	17.9
BBA-com + A	8.0	8.1
2AB-com1	−1.8	−1.0
2AB-com2	−0.9	−0.3
2AB-com3	6.5	7.0
DADB	−3.5	−3.3
2AB-p1 + H_2	−14.8	−16.7
2AB-p2 + A + H_2	2.0	0.2
DBA-ts + A	19.9	20.4
2AB-ts1	11.0	12.4
2AB-ts2	25.0	25.8
2AB-ts3	26.7	27.8
2AB-ts4	30.3	30.7
2AB-ts5	37.2	38.2
2AB-ts6	38.5	38.5

[a] Calculated at the CCSD(T) level using MP2/aVTZ-optimized geometries and scaled MP2/aVDZ ZPE corrections.

TABLE 6: CCSD(T) Relative Energies (kcal/mol) of Transition State and Equilibrium Structures for H_2 Release from the Ion Pair, $[BH_4^+][NH_3BH_2NH_3^-]$, DADB[a]

structures	aVDZ	aVTZ
2AB	0.0	0.0
DADB	−3.5	−3.3
DADB-p1 + H_2	−7.8	−9.3
DADB-p2 + H_2	8.1	7.4
DADB-p3 + H_2	−19.1	−20.8
DADB-ts1	17.2	17.2
DADB-ts2	48.3	47.8
DADB-p1-ts + H_2	−5.9	−7.3

[a] Calculated at the CCSD(T) level using MP2/aVTZ-optimized geometries and scaled MP2/aVDZ ZPE corrections.
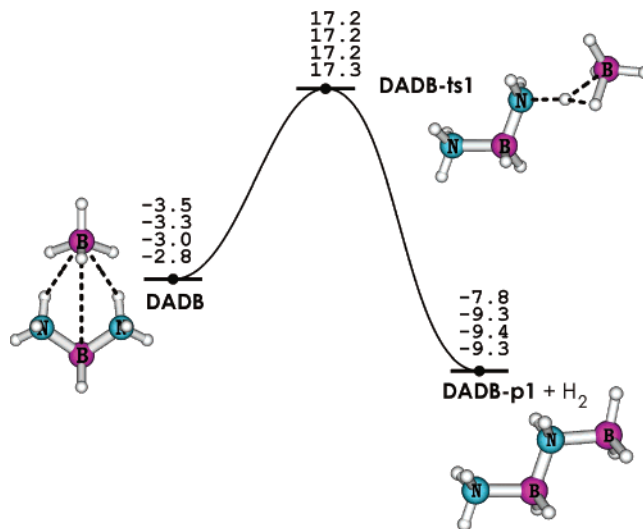

Figure 10. Schematic potential energy profiles in kcal/mol showing the reaction pathway for H_2 release from **DADB**, calculated with the CCSD(T) method using four basis sets including zero-point corrections. The energies are from top to bottom: aVDZ, aVTZ, aVQZ, and CBS.

TABLE 7: CCSD(T) Relative Energies (kcal/mol) of Transition State and Equilibrium Structures for H_2 Release from the Ion Pair, $[NH_4^+][BH_3NH_2BH_3^-]$, IonP-N[a]

structures	aVDZ	aVTZ
2AB	0.0	0.0
IonP-N	2.3	2.7
IonP-N + H_2	14.6	14.2
IonP-N-ts1	20.3	20.4
IonP-N-ts2	59.0	58.7

[a] Calculated at the CCSD(T) level using MP2/aVTZ-optimized geometries and scaled MP2/aVDZ ZPE corrections.

in **2AB-ts1** or can break apart, forming BH_3 and NH_3 to catalyze the process as in **2AB-ts2** and **2AB-ts3**.

In addition, it is useful to compare **2AB-ts1** and **2AB-ts3** (Figure 7), which only differ by the orientation of the NH_3 relative to the effectively separated BH_3. In **2AB-ts1**, the NH_3 interacts with the noncovalently bonded BH_3 and connects **BBA-com** to 2 **AB**. In **2AB-ts3**, the NH_3 approaches the BH_3 of the monomer from the opposite side, leading to transfer of the H on the BH_3 to form BH_4^- and $NH_3BH_2NH_3^+$, the components of **DADB**. Thus, the orientation of the incoming NH_3 controls which part of the potential energy surface is accessed.

Reaction Pathways for H_2 Release from Ion Pair Isomers. We now examine the production of H_2 from the ion pairs **DADB** and **IonP-N**. Figure 9 displays geometrical parameters of five relevant TS's. Calculated relative energies obtained at the CCSD(T) level with the aVDZ and aVTZ basis sets are given in Tables 5, 6, and 7. The energy profiles at the CCSD(T)/aVTZ level are shown in Figures 10, 11, and 12. Total and ZPEs are tabulated in Table S-3 of the Supporting Information.

DADB-ts1 is the TS for the generation of one H_2 molecule from **DADB** (Figure 9). For this reaction channel, results up to the CCSD(T)/CBS level are compared in Table 2 and illustrated in Figure 10. Again, the energies obtained using the aVTZ basis set are very similar to the CBS values. As hydrogen transfer occurs, the BH_4 moiety rotates around a NH_3 group to yield a

trans configuration for **DADB-ts1**. IRC calculations confirmed the connection between **DADB** and the product **DADB-p1**. The B—H bond of the BH_4^- moiety only lengthens by 0.09 Å, whereas the N—H bond is substantially longer by 0.37 Å. The forming H_2 has a distance of 0.968 Å at **DADB-ts1**, longer than the values found above. H_2 production through this TS is of much lower energy than the one described above, with an energy barrier of only 20.1 kcal/mol. The product generated from **DADB** is the chain molecule $NH_3BH_2NH_2BH_3$ **DADB-p1**. The reaction is slightly exothermic, −6.5 kcal/mol with respect to **DADB** (CBS results, Figure 10). The trans chain (linear) **DADB-p1** found by IRC calculations as the primary product does not correspond to the lowest-lying conformation of the molecule. As given in reactions 4 and 5, the gauche (coiled) conformer is 12.2 kcal/mol more stable than the trans conformer, due to the presence of stabilizing B—H···H—N interactions[42] (11.5 kcal/mol at the CCSD(T)/aVTZ + ZPE level, cf. Figure 11). The conversion of the trans **DADB-p1** to the gauche form **DADB-p3** described in Figure 11 is however a low-energy process, with a barrier of rotation of 2.0 kcal/mol around the central B—N bond involving the TS **DADB-p1-ts** (Figure 9).

There is another pathway for generating H_2 from **DADB** involving the TS **DADB-ts2** leading to the ion pair **DADB-p2**. As shown in Figure 11, **DADB-p2** is 16.7 kcal/mol less stable than **DADB-p1**, and **DADB-ts2** lies 30.6 kcal/mol higher in energy than **DADB-ts1**. Therefore, the ion pair $[BH_4^-][NH_3BH_2NH_3^+]$ undergoes preferentially H_2 eliminations overcoming an energy barrier of 20.5 kcal/mol via **DADB-ts1** (Figure 11). This result is consistent with the experimental finding that **DADB**, gener-
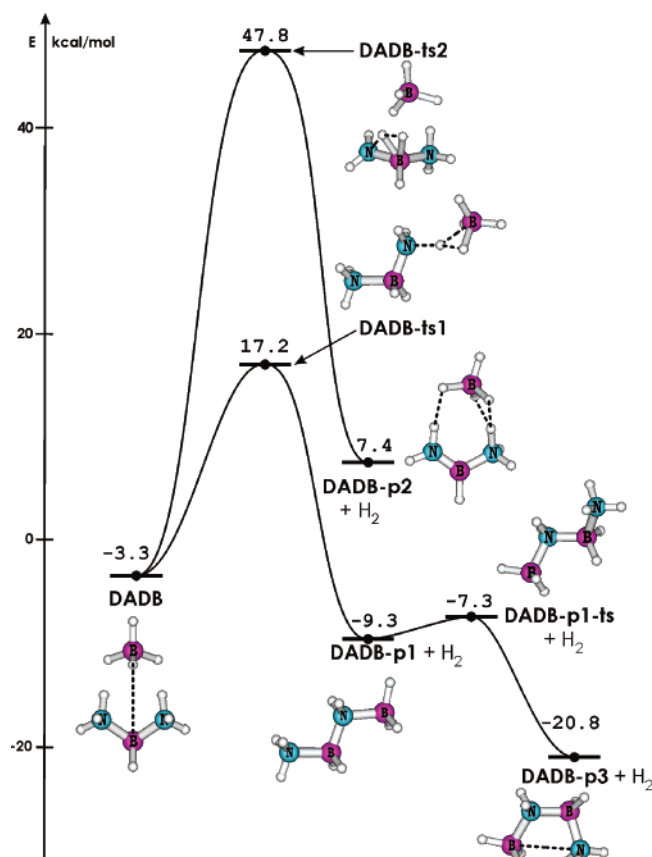
Figure 11. Schematic energy profiles illustrating the different reaction pathways for H_2 release from **DADB.** Relative energies in kcal/mol were obtained from CCSD(T)/aVTZ + ZPE calculations.
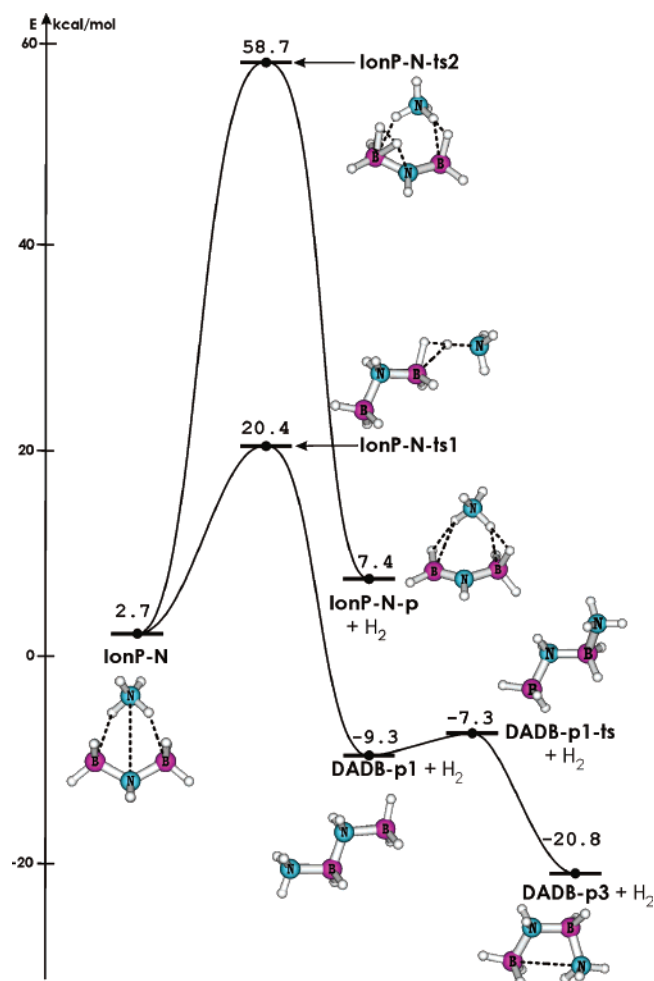

Figure 12. Schematic energy profiles illustrating two different reaction pathways for H_2 release from **IonP-N**. Relative energies in kcal/mol were obtained from CCSD(T)/aVTZ + ZPE calculations.

ated following a seeding of $(\mathbf{AB})_2$ dimer, releases H_2 under mild temperatures.[14]

IonP-N-ts1 and **IonP-N-ts2** link the ion pair **IonP-N** $[NH_4{}^+][BH_3NH_2BH_3{}^-]$ with the H_2 release products (Figure 12). The trans chain product **DADB-p1** from the reaction involving **IonP-N-ts1**, whose geometry is shown in Figure 9, turns out to be the same as that from **DADB**. The shape of this TS is similar to that of **DADB-ts1**, in which a trans conformation results from a migration of the NH_4 moiety. The H_2 formation arises equally from a B—H···H—N interaction. The energy barrier associated with the process **IonP-N** → **IonP-N-ts1** is 17.7 kcal/mol, 2.8 kcal/mol smaller than that of **DADB** proceeding through **DADB-ts1** (Figure 12 at the same level of theory). **IonP-N-ts2** is too high an energy process to be considered.

Despite many attempts, we were not successful in identifying a direct reaction pathway linking the neutral dimer **dim** with either ion pair **DADB** or **IonP-N**, apart from those shown in Figure 8. There is a path to DADB that involves breaking the dimer interaction and starting from two monomers. The first step to form the two monomers requires 14.0 kcal/mol. A second step is to break the B—N bond, which requires an additional 25.9 kcal/mol. An additional energy of only 1.9 kcal/mol is required to reach the value of 41.8 kcal/mol to reach TS **2AB-ts3** leading to **DADB**. The actual reaction proceeds through the intermediate **BBA-com** + NH_3, which is reached by a barrier of 12.4 kcal/mol starting from 2 **AB**. The energy barrier of 41.8 kcal/mol is a few kcal/mol smaller than the values of 44.5 and 50.0 kcal/mol for one-step elimination of one H_2 (Figure 5) and two H_2 molecules (Figure 5), respectively, from **dim**.

Thermal decomposition of **AB** has been experimentally shown to yield H_2 at mild temperatures ($T \leq 80$ °C).[5] Our results

suggest that H_2 release from ammonia borane under these conditions does not proceed through the hydrogen-bonded dimer **dim**. The dimer **dim** can generate one or two H_2 molecules through direct pathways having energy barriers ranging from 44.5 to 50.0 kcal/mol with respect to the dimer (Figure 5). Instead, our results show that H_2 can be released more readily if an ion pair is formed. Although **DADB** is 10.6 kcal/mol less stable than **dim**, the pathway for H_2 elimination from **DADB** is characterized by a smaller energy barrier of 20.1 kcal/mol. In the gas phase, the path that converts **dim** to **DADB** is has a barrier of 41.8 kcal/mol (through **2AB-ts3**). Such a conversion could be a lower-energy process in condensed media,[15] so the barrier to lose H_2 from the dimer would be reduced to 30.7 kcal/mol in the absence of additional solid-state effects.

The second ion pair $[NH_4{}^+][BH_3NH_2BH_3{}^-]$ **IonP-N** is 16.4 kcal/mol less stable than the neutral dimer and has a smaller energy barrier of 17.7 kcal/mol for H_2 elimination. Again, the barrier for loss of H_2 starting from **dim** via **IonP-N** would be 34.1 kcal/mol, slightly higher than proceeding through **DADB**. These barriers are both below the unimolecular loss of H_2 from BH_3NH_3.[13] We found that the decomposition of both ion pairs produces the chain $BH_3NH_2BH_2NH_3$ structure, just as observed in the solid-state and ionic liquid studies.[15,8b]

Concluding Remarks

In the present study, we have investigated the reaction pathways and the molecular mechanisms for H_2 release from

Release of H$_2$ from (BH$_3$NH$_3$)$_2$

J. Phys. Chem. A, Vol. 111, No. 36, 2007 **8855**

dimers of ammonia borane. In addition to the more conventional neutral dimer, we have found two ion pair isomers. One of them is **DADB**, which was experimentally identified following seeding of the neutral (**AB**)$_2$ dimer. The most stable gaseous phase dimer **dim** results from a head-to-tail cyclic interaction and is stabilized by 14.0 kcal/mol with respect to the two **AB** monomers. The neutral dimer **dim** could generate one H$_2$ molecule through direct pathways having energy barriers near 45 kcal/mol, substantially higher than for loss from the monomer. The pathway for loss of two H$_2$ molecules is even higher near 50 kcal/mol. Reactions of two monomers and of one monomer with separated BH$_3$ and NH$_3$ lead to either **DADB** or H$_2$ formation with energy barriers of ∼26−28 kcal/mol. Successive additions of two NH$_3$ molecules to B$_2$H$_6$ also lead to **DADB** via an energetically lower-lying TS. Although **DADB** is 10.6 kcal/mol less stable than **dim**, the pathway for H$_2$ elimination from **DADB** is characterized by a smaller energy barrier of ∼21 kcal/mol. **IonP-N** is 16.4 kcal/mol less stable than the neutral dimer, and the energy barrier for loss of H$_2$ is reduced to ∼18 kcal/mol. The chain molecule BH$_3$NH$_2$BH$_2$-NH$_3$, a key precursor for the formation of borane amine oligomers, was predicted to be generated when H$_2$ is lost from either ion pair but not from the more stable **dim**. Our results are consistent with the experimental observation that seeding of BH$_3$NH$_3$ produces the diammoniate of diborane.

Supporting Information Available: CCSD(T) total energies, MP2 ZPEs, Cartesian coordinates of the MP2/aVTZ-optimized geometries, and atomization energy components for the ion pairs and the ions BH$_3$NH$_2$BH$_3$$^-$ and NH$_3$BH$_2$NH$_3$$^+$ and figures showing important MP2/aVTZ geometry parameters of the transition structures **dim-ts6**, **dim-ts7**, and **dim-ts8** for the release of one H$_2$ molecule from **dim** and the various products. This material is available free of charge via the Internet at http://pubs.acs.org.

References and Notes

(1) (a) *Basic Energy Needs for the Hydrogen Economy*; Dressalhaus, M., Crabtree, G., Buchanan, M., Eds.; Basic Energy Sciences, Office of Science, U. S. Department of Energy: Washington, DC, 2003. (b) Maelund, A. J.; Hauback, B. C. In *Advanced Materials for Energy Conversion II*; Chandra, D., Bautista, R. G., Schlapbach, L., Eds.; The Minerals, Metals and Materials Society: Warrendale, PA 2004.

(2) Parry, R. W.; Schultz, D. R.; Girardot, P. R. *J. Am. Chem. Soc.* **1958**, *80*, 1.

(3) Sorokin, V. P.; Vesnina, B. I.; Klimova, N. S. *Russ. J. Inorg. Chem.* **1963**, *8*, 32.

(4) (a) Geanangel, R. A.; Wendlandt, W. W. *Thermochim. Acta* **1985**, *86*, 375. (b) Sit, V.; Geanangel, R. A.; Wendlandt, W. W. *Thermochim. Acta* **1987**, *113*, 379. (c) Wang, J. S.; Geanangel, R. A. *Inorg. Chim. Acta* **1988**, *148*, 185.

(5) (a) Wolf, G.; van Miltenburg, R. A.; Wolf, U. *Thermochim. Acta* **1998**, *317*, 111. (b) Wolf, G.; Baumann, J.; Baitalow, F.; Hoffmann, F. P.

Thermochim. Acta **2000**, *343*, 19. (c) Baitalow, F.; Baumann, J.; Wolf, G.; Jaenicke-Robler, K.; Leitner, G. *Thermochim. Acta* **2002**, *391*, 159.

(6) Dixon, D. A.; Gutowski, M. *J. Phys. Chem. A* **2005**, *109*, 5129.

(7) Grant, D.; Dixon, D. A. *J. Phys. Chem. A* **2005**, *109*, 10138.

(8) (a) Yoon, C. W.; Sneddon, L. G. *J. Am. Chem. Soc.* **2006**, *128*, 13992. (b) Bluhm, M. E.; Bradley, M. G.; Butterick, R., III.; Kusari, U.; Sneddon, L. G. *J. Am. Chem. Soc.* **2006**, *128*, 7748.

(9) (a) Gutowska, A.; Li, L.; Shin, Y.; Wang, C. M.; Li, X. S.; Linehan, J. C.; Smith, R. S.; Kay, B. D.; Schmid, B.; Shaw, W.; Gutowski, M.; Autrey, T. *Angew. Chem., Int. Ed.* **2005**, *44*, 3578. (b) Stephans, F. H.; Baker, R. T.; Matus, M. H.; Grant, D. J.; Dixon, D. A. *Angew. Chem., Int. Ed.* **2007**, *46*, 641.

(10) Clark, T. J.; Russell, C. A.; Manners, I. *J. Am. Chem. Soc.* **2006**, *128*, 9682.

(11) Denny, M. C.; Pons, V.; Hebden, T. J.; Heinekey, D. M.; Goldberg, K. I. *J. Am. Chem. Soc.* **2006**, *128*, 12048.

(12) (a) McKee, M. L, *J. Phys. Chem.* **1992**, *96*, 5380. (b) Sakai, S. *Chem. Phys. Lett.* **1994**, *217*, 288. (c) Sakai, S. *J. Phys. Chem.* **1995**, *99*, 9080. (d) Li, Q. S.; Zhang, J.; Zhang, S. *Chem. Phys. Lett.* **2005**, *404*, 100.

(13) (a) Nguyen, M. T.; Nguyen, V. S.; Matus, M. H.; Gopakumar, G.; Dixon, D. A. *J. Phys. Chem. A* **2007**, *111*, 679. (b) Matus, M. H.; Nguyen, M. T.; Dixon, D. A. *J. Phys. Chem. A* **2007**, *111*, 1726.

(14) Aardahl, C.; Autrey, T.; Gutowski, M.; Linehan, J.; Rassat, S.; Camaioni, D.; Rector, D.; Shaw, W.; Stowe, A.; Smith, S.; Heldebrant, D.; Shin, Y.; Li, L.; Li, J. *Annual Progress Report: Chemical Hydrogen Storage Center*; Pacific Northwest National Laboratory: Richmond, WA, May 16, 2006. http://www.hydrogen.energy.gov/pdfs/progress06/iv_b_4b_aardahl.pdf. Heldebrant, D. J.; Linehan, J. C.; Camaioni, D. M.; Rassat, S. D.; Zheng, F.; Autrey, T. *Am. Chem. Soc., Div. Fuel Chem.* **2007**, *52* (2), in press.

(15) Stowe, A. C.; Shaw, W. J.; Linehan, J. C.; Schmid, B.; Autrey, T. *Phys. Chem. Chem. Phys.* **2007**, *9*, 1831.

(16) Mayer, E. *Inorg. Nucl. Chem. Lett.* **1973**, *9*, 343.

(17) (a) Stock, A.; Pohland, E. *Chem. Ber.* **1926**, *59*, 2215. (b) Schlesinger, H. I.; Burg, A. B. *J. Am. Chem. Soc.* **1938**, *60*, 290.

(18) Frisch, M. J.; Trucks, G. W.; Schlegel, H. B.; Scuseria, G. E.; Robb, M. A.; Cheeseman, J. R.; Montgomery, J. A., Jr.; Vreven, T.; Kudin, K. N.; Burant, J. C.; Millam, J. M.; Iyengar, S. S.; Tomasi, J.; Barone, V.; Mennucci, B.; Cossi, M.; Scalmani, G.; Rega, N.; Petersson, G. A.; Nakatsuji, H.; Hada, M.; Ehara, M.; Toyota, K.; Fukuda, R.; Hasegawa, J.; Ishida, M.; Nakajima, T.; Honda, Y.; Kitao, O.; Nakai, H.; Klene, M.; Li, X.; Knox, J. E.; Hratchian, H. P.; Cross, J. B.; Bakken, V.; Adamo, C.; Jaramillo, J.; Gomperts, R.; Stratmann, R. E.; Yazyev, O.; Austin, A. J.; Cammi, R.; Pomelli, C.; Ochterski, J. W.; Ayala, P. Y.; Morokuma, K.; Voth, G. A.; Salvador, P.; Dannenberg, J. J.; Zakrzewski, V. G.; Dapprich, S.; Daniels, A. D.; Strain, M. C.; Farkas, O.; Malick, D. K.; Rabuck, A. D.; Raghavachari, K.; Foresman, J. B.; Ortiz, J. V.; Cui, Q.; Baboul, A. G.; Clifford, S.; Cioslowski, J.; Stefanov, B. B.; Liu, G.; Liashenko, A.; Piskorz, P.; Komaromi, I.; Martin, R. L.; Fox, D. J.; Keith, T.; Al-Laham, M. A.; Peng, C. Y.; Nanayakkara, A.; Challacombe, M.; Gill, P. M. W.; Johnson, B.; Chen, W.; Wong, M. W.; Gonzalez, C.; Pople, J. A. *Gaussian 03*, revision C.01; Gaussian, Inc.: Wallingford, CT, 2004.

(19) Deegan, M. J. O.; Dobbyn, A. J.; Eckert, F.; Hampel, C.; Hetzer, G.; Knowles, P. J.; Korona, T.; Lindh, R.; Lloyd, A. W.; McNicholas, S. J.; Manby, F. R.; Meyer, W.; Mura, M. E.; Nicklass, A.; Palmieri, P.; Pitzer, R.; Rauhut, G.; Schütz, M.; Schumann, U.; Stoll, H.; Stone, A. J.; Tarroni, R.; Thorsteinsson, T.; Werner, H.-J. *MOLPRO: A Package of Ab Initio Programs*, version 2002.6; Universität Stuttgart and University of Birmingham: Stuttgart, Germany, and Birmingham, United Kingdom, 2002.

(20) Pople, J. A.; Seeger, R.; Krishnan, R. *Int. J. Quantum Chem., Quantum Chem. Symp.* **1977**, *11*, 149.

(21) (a) Dunning, T. H., Jr. *J. Chem. Phys.* **1989**, *90*, 1007. (b) Kendall, R. A.; Dunning, T. H., Jr.; Harrison, R. J. *J. Chem. Phys.* **1992**, *96*, 6796.

(22) Gonzalez, C.; Schlegel, H. B. *J. Chem. Phys.* **1989**, *90*, 2154.

(23) (a) Becke, A. D. *J. Chem. Phys.* **1993**, *198*, 5648. (b) Lee, C.; Yang, W.; Parr, R. G. *Phys. Rev.* **1988**, *37*, 785.

(24) (a) Cizek, J. *Adv. Chem. Phys.* **1969**, *14*, 35. (b) Purvis, G. D.; Bartlett, R. J. *J. Chem. Phys.* **1982**, *76*, 1910. (c) Pople, J. A.; Head-Gordon, M.; Raghavachari, K. *J. Chem. Phys.* **1987**, *87*, 5968.

(25) Peterson, K. A.; Woon, D. E.; Dunning, T. H., Jr. *J. Chem. Phys.* **1994**, *100*, 7410.

(26) Nguyen, V. S.; Matus, M. H.; Nguyen, M. T.; Dixon, D. A. *J. Phys. Chem. A* **2007**, *111*, 9603.

(27) Jenkins, H. D. B.; Tudela, D.; Glaser, L. *Inorg. Chem.* **2002**, *41*, 2364.

(28) Mallouk, T. E.; Rosenthal, G. L.; Müller, G.; Busasco, R.; Bartlett, N. *Inorg. Chem.* **1984**, *23*, 3167.

(29) (a) Zhan, C. G.; Dixon, D. A. *J. Phys. Chem. A* **2001**, *105*, 11534. (b) Zhan, C. G.; Chipman, D. M. *J. Chem. Phys.* **1998**, *109*, 10543.

(30) Merino, G.; Bakhmutov, V. I.; Vela, A. *J. Phys. Chem. A* **2002**, *106*, 8491.

(31) Meng, Y.; Zhou, Z.; Duan, C.; Wang, B.; Zhong, Q. *J. Mol. Struct.: (THEOCHEM)* **2005**, *713*, 135.

8856 *J. Phys. Chem. A, Vol. 111, No. 36, 2007*

Nguyen et al.

(32) Richardson, T.; Gala, S.; Crabtree, R. *J. Am. Chem. Soc.* **1995**, *117*, 12875.

(33) Klooster, W. T.; Koetzle, T. F.; Siegbahn, P. E. M.; Richardson, T. B.; Crabtree, R. H. *J. Am. Chem. Soc.* **1999**, *121*, 6337.

(34) Cramer, C. J.; Gladfelter, Q. L. *Inorg. Chem.* **1997**, *36*, 5358.

(35) Popelier, P. L. A. *J. Phys. Chem. A* **1998**, *102*, 1873.

(36) (a) Kulkarni, S. *J. Phys. Chem. A* **1998**, *102*, 7704. (b) Kulkarni, S. *J. Phys. Chem. A* **1999**, *103*, 9330.

(37) Li, J.; Zhao, F.; Jing, F. *J. Chem. Phys.* **2002**, *116*, 25.

(38) Dillen, J.; Verhoeven, P. *J. Phys. Chem. A* **2003**, *107*, 2570.

(39) Kar, T.; Scheiner, S. *J. Chem. Phys.* **2003**, *119*, 1473.

(40) Clustelcean, R.; Dreger, Z. *J. Phys. Chem. B* **2003**, *107*, 9231.

(41) Morrison, C. A.; Siddick, M. M. *Angew. Chem., Int. Ed.* **2004**, *43*, 4780.

(42) Matus, M. H.; Anderson, K. D.; Camaioni, D. M.; Autrey, T.; Dixon, D. A. *J. Phys. Chem. A* **2007**, *111*, 4411.

(43) (a) Peterson, K. A.; Dunning, T. H., Jr. *J. Chem. Phys.* **2002**, *117*, 10548. (b) Woon, D. E.; Dunning, T. H., Jr. *J. Chem. Phys.* **1993**, *98*, 1358.

(44) (a) Peterson, K. A.; Dunning, T. H., Jr. *J. Chem. Phys.* **2002**, *117*, 10548. (b) Woon, D. E.; Dunning, T. H., Jr. *J. Chem. Phys.* **1993**, *98*, 1358.

(45) Moore, C. E. *Atomic Energy Levels*; National Bureau of Standards Circular 467; U. S. Department of Commerce, National Bureau of Standards: Washington, DC, 1949.

(46) Chase, M. W., Jr. NIST-JANAF Tables (4th Edition). *J. Phys. Chem. Ref. Data* **1998**, Monograph 9 (Suppl. 1). See also *NIST Chemistry WebBook*; Linstrom, P. J.; Mallard, W. G., Eds.; NIST Standard Reference Database Number 69; National Institute of Standards and Technology: Gaithersburg MD, 2005 (http://webbook.nist.gov/chemistry/).

(47) (a) Ruscic, B.; Mayhew, C. A.; Berkowitz, J. *J. Chem. Phys.* **1988**, *88*, 5580. (b) Storms, E.; Mueller, B. *J. Phys. Chem.* **1977**, *81*, 318. (c) Ochterski, J. W.; Petersson, G. A.; Wiberg, K. B. *J. Am. Chem. Soc.* **1995**, *117*, 11299.

(48) Curtiss, L. A.; Raghavachari, K.; Redfern, P. C.; Pople, J. A. *J. Chem. Phys.* **1997**, *106*, 1063.

(49) Nguyen, V. S.; Matus, M. H.; Nguyen, M. T.; Dixon, D. A. *J. Phys. Chem. A*, to be published.